Proceedings of the
2007 IEEE Intelligent Vehicles Symposium
Istanbul, Turkey, June 13-15, 2007

Control Solutions for Hybrid Solar Vehicle Fuel Consumption Minimization

Zsuzsa Preitl, Peter Bauer, Balazs Kulcsar, Gianfranco Rizzo, Jozsef Bokor

Abstract— **Hybrid electric vehicles (HEVs) gain more and more attention, as they represent a more environmental friendly alternative to conventional vehicles. If combined with photovoltaic panels, they can lead to further reduction of emissions. The paper focuses on a solution for minimizing the fuel consumption in a series hybrid solar vehicle (HSV). After briefly introducing the model, first a global optimum in fuel consumption is presented using dynamic programming, as a reference value. As a real-time control strategy, Model Predictive Control (MPC) is considered. A fuel consumption equivalent quantity is defined which is used for calculating the fuel needed to bring the battery state of charge to a starting value (set in this case for 0.7 in relative units). For different values of the MPC tuning parameters simulations are performed using the urban section of the New European Drive Cycle. Conclusions based on the simulations are presented.**

I. Introduction

HYBRID electric vehicles (HEVs) are combining multiple main energy sources, usually consisting in a conventional fuel tank and a battery. By adding a photovoltaic panel, a Hybrid Solar Vehicle (HSV) is obtained. Different types of HSV architectures can be used, depending on the actual requirements [1],[2]. These are differentiated through their drivetrain structures, the basic structures are: series, parallel, series/parallel and complex hybrids. For hybrid solar vehicles, the series structure is receiving increasing attention due to its capability to interact with grid within the plug-in hybrid concept [3]. In the paper the series structure is used, proving to be optimal for urban drive, this structure has been recently adopted for modelling purposes on HSVs [4] and for some prototypes [5].

The paper is structured as follows: first the main components are briefly presented, based on [6], resulting in a linearized mathematical model of the HSV. Section III presents Dynamic Programming (DP) results for fuel consumption minimization. In section IV a fuel equivalent is defined, based on the fuel consumption evolution during the drive cycle. This measure allows the calculation of an equivalent of fuel amount needed (or in excess) for establishing a battery state of charge level of 0.7 (in relative units). Section V presents Model Predictive Control (MPC) as a practice oriented solution. Simulations were performed for different controller parameters. The last section draws conclusions based on the simulation results.

Manuscript received on January 15, 2007.

Zsuzsa Preitl and Peter Bauer are with the Dept. of Control and Transport Automation, Budapest University of Technology and Economics, H-1111 Budapest, Hungary (phone: +36-1-4633089; fax: +36-1-4633087; email: preitl@mail.bme.hu).

Gianfranco Rizzo is with the Dept. of Mechanical Engineering, University of Salerno, 84084 Fisciano (SA), Italy (e-mail: grizzo@unisa.it).

Balazs Kulcsar and Jozsef Bokor are with the Computer and Automation Research Institute, Hungarian Academy of Sciences, H-1518 Budapest, Hungary (e-mail: bokor@sztaki.hu).

II. Mathematical Model of the HSV

A. HSV architecture aspects

The general architecture of a series HSV is depicted in figure 1 (main components and power distribution).

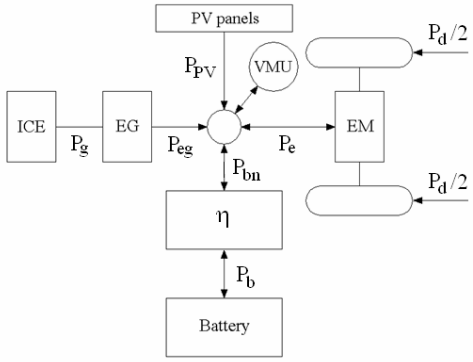

Fig. 1. Series hybrid vehicle basic architecture

A fuel minimization oriented modelling assumes the following main components: the electric motor (EM) which drives the wheels or works as a generator during regenerative braking; the electric generator (EG) which delivers electrical energy for the EM; the photovoltaic (PV) panel and a battery. The EG is in rigid connection with the internal combustion engine (ICE). The vehicle management unit (VMU) controls and coordinates the components. The power balance is presented in more detail in section III.

B. Brief component modelling

The EMs considered for electric vehicles are either DC motors or brushless DC motors [7],[8]. In this paper a brushless DC motor (BLDC) is considered which can be used both as motor and as generator. The BLDC's operating range is divided into four quadrants: forward motoring, forward breaking, reverse motoring and reverse braking. A qualitative modelling is used, namely the steady-state speed-torque curves $M = f(\omega; U - parameter)$, described by the following relation:

$$M = \frac{K_t}{1.1R_m}[U - K_e\omega] \quad (1)$$

where M is the torque, ω is the angular velocity, U is voltage, R_m is resistance, K_t, K_e, are the electromechanical and the electromagnetic constants of the machine.

The power balance between the electrical (P_{el}) and mechanical powers (P_m) is also taken into account:

$$P_{el}=P_m/\eta_{EM} \tag{2}$$

More details regarding the model and numerical data can be found in [6].

The battery model used in the paper is a relatively complex model, considering the battery a real voltage generator [9], which considers the change in open circuit voltage when battery state of charge (SOC) changes. The literature contains also a large variety of other models, from simple ones to complex models [10],[11]. The efficiency of the battery is considered in a non-linear manner (see equation (3) and symbolised with η for simplicity in figure 2, which depicts the overall structure of the battery model).

$$P_b = \frac{1-\sqrt{1-6\cdot 10^{-5}\cdot P_{bn}}}{3\cdot 10^{-5}} \tag{3}$$

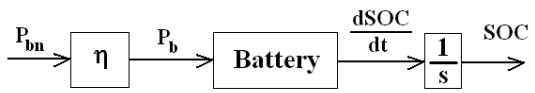

Fig. 2. Battery simulation structure

The state of charge (SOC) is defined in relative units, namely between 0 (empty) and 1 (full charge). A condition is imposed so that the SOC stays between the values of (0.6 … 0.8), and the starting value is 0.7. More details regarding the battery model can be found in [6]. Here also the hypothesis is accepted according to which the final value of the SOC be as close as possible to the starting value of 0.7.

The choice of the PV panel does not depend on the other components. It is modelled with the following equation:

$$P_{PV} = U_{opt}(\lambda)\cdot K(\lambda)\cdot\left(1-e^{\frac{U_{opt}(\lambda)-U_{\max}(\lambda)}{T_U(\lambda)}}\right)\cdot \cdot(1+K_P(T-25)) \tag{4}$$

Here U_{opt} is the output voltage value at the maximum power point, $U_{\max}$ is the maximum possible output voltage, K and T_U are parameters, λ is the irradiation value, T is the cell temperature. Although photovoltaic panels should be controlled separately by MPPT (Maximum Power Point Tracking) methods in order to maximize the net energy [12], PV power itself cannot be considered as a control variable.
The electric generator (EG) and internal combustion engine (ICE) should be fitted to the electric motor and to each other (in the maximum efficiency region). This way the EG can be described by a single characteristic curve, between input mechanical and output electrical power, see figure 3.

The description of ICE is possible in a similar way considering the maximum efficiency working line. The fuel map of the proper ICE (which can satisfy the EG input power needs) is depicted in figure 4.

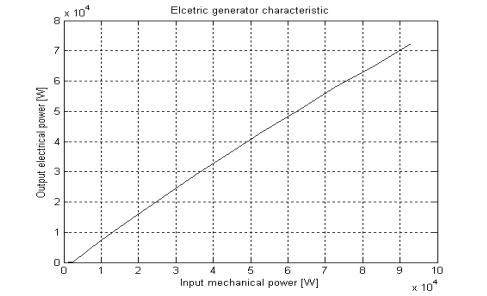

Fig. 3. Characteristic curve of electric generator

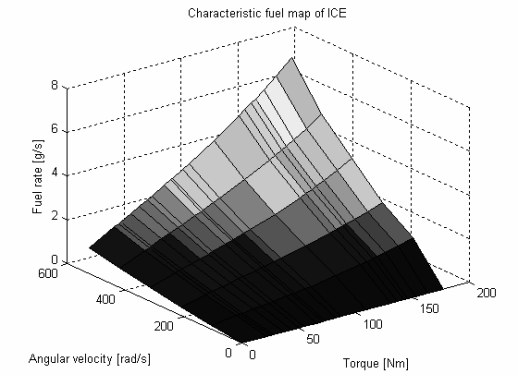

Fig.4. Characteristic fuel map of the ICE

C. Plant model and drive cycle used

The model of the plant resulted in a non-linear model [6], where the elements were modelled each as presented above, and connected according to figure 1. Also first order lag elements were introduced for catching the dynamics of the ICE and EM, with adequate time constants. A Simulink model was built based on this, and for controller design a linearization was performed around a working point, using the Matlab function *linmod2*. For simulation, the non-linear model was used for the plant. The inputs, outputs and states of the mathematical model are as follows:

- Inputs: - u_1: ICE power,
  - u_2: Battery nominal power;
- State variables: - x_1: state of dynamics of ICE,
  - x_2: SOC,
  - x_3: state of dynamics of EM;
- Measured disturbance input: - d_m: PV panel power.
- Outputs: - o_1: Drive power,
  - o_2: SOC,
  - o_3: Fuel rate;

$$\begin{bmatrix}x_1(k+1)\\x_2(k+1)\\x_3(k+1)\end{bmatrix}=\begin{bmatrix}0.3679 & 0 & 0\\0 & 1 & 0\\0 & 0 & 0.9048\end{bmatrix}\begin{bmatrix}x_1(k)\\x_2(k)\\x_3(k)\end{bmatrix}+ +\begin{bmatrix}3.78\cdot 10^{-6} & 6.321\cdot 10^{-4}\\0 & -1.517\cdot 10^{-11}\\2.638\cdot 10^{-7} & 0\end{bmatrix}\begin{bmatrix}u_1(k)\\u_2(k)\end{bmatrix}+ +\begin{bmatrix}6.321\cdot 10^{-4}\\0\\0\end{bmatrix}d_m(k) \tag{5}$$

$$\begin{bmatrix} y_1(k) \\ y_2(k) \\ y_3(k) \end{bmatrix} = \begin{bmatrix} 800 & 0 & 0 \\ 0 & 1 & 0 \\ 0 & 0 & 100 \end{bmatrix} \begin{bmatrix} x_1(k) \\ x_2(k) \\ x_3(k) \end{bmatrix}$$

The linearized discrete time state-space model of the plant, using a sampling time of $T_s=0.001$ sec, is described with (5). The numerical data is taken from the literature [9], and presented in more detail in [6] and [13].

The system is both controllable and observable. Constraints act upon the system inputs and outputs, enumerated in equations (6).

$$\begin{cases} 0 \le u_1 \le 93000 \\ -26000 \le u_2 \le 14000 \\ -40000 \le y_1 \le 58000 \\ 0.6 \le y_2 \le 0.8 \\ 0 \le y_3 \le 7.3 \end{cases} \quad (6)$$

The PV power is treated as a measured disturbance, depending on the actual irradiation value.

In order to test the system and offer comparable results, in the paper the urban part of the New European Drive Cycle (NEDC) is considered [10], that means the first 800 seconds. The time-velocity characteristics of the urban part of NEDC are depicted in figure 5.

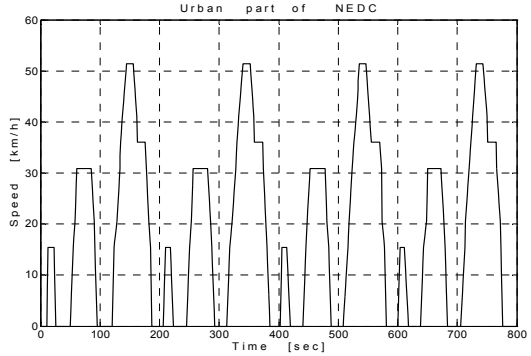

Fig. 5. Urban part of the New European Drive Cycle

III. Dynamic Programming Solution to Fuel Consumption Minimization

Dynamic programming (DP) is suitable for obtaining the global optimum of a problem, resulting in an optimal input sequence applied to the plant input. Unfortunately, DP cannot be applied in real-time, since it requires a-priori knowledge of all reference signals and disturbances acting on the entire duration of the drive. Still DP is very useful since it delivers a reference solution, the global optimum, and all other control solutions can be compared to it.

The aim of the paper is fuel consumption minimization over a certain time horizon, in this case for the urban part of the NEDC, realized through a proper balancing of the energy sources. The electric motor's power requirements can be satisfied by the electric generator, battery and PV panel [14].

The power balance of the system is described by the following equation:

$$P_e = P_{eg} + P_{bn} + P_{PV} \quad (7)$$

In this case P_{eg} electric generator power and P_{bn} battery nominal power are the control variables. P_e electric motor power can be calculated from P_d drive power need, considering the characteristics of the EM. P_{eg} and P_{bn} are influenced by the controller, being the control signals of the system. The power balance of the system is also depicted in figure 1. The nominal values for the considered powers are: $P_{e,n}=40$ kW, $P_{PV,n}=600$ W, $P_{ICE,n}=67$ kW, $P_{eg,n}=55$ kW.

The calculations are performed considering the possible SOC values at every time step, which can be achieved according to the constraint, $SOC(0) \equiv SOC(end)$, and the minimal and maximal allowed SOC values (0.6 and 0.8, respectively) [15]. A more detailed description of DP used for HSV can be found in [13].

After calculating the optimal input sequence P_{bn} and deriving P_{eg} out of it based on (7), the optimal solution in fuel consumption minimization gives the following reference values:

- Total fuel consumed: 200.2299g
- Final SOC: 0.7

IV. Fuel Consumption Equivalent Definition

For fuel consumption minimization different control strategies can be applied, as alternatives to DP, and their performances compared to each other. If after a drive cycle the SOC differs from 0.7, a fuel equivalent can be defined to characterize in terms of fuel needed (or excess) the "distance" from this SOC value. In the paper the following concept was applied: during the drive cycle the time mean integral of the fuel amount consumed only for charging the battery is calculated.

Starting from equation (7) and figure 1, if $P_{bn}<0$ the battery is charged. Suppose the PV panel delivers constant energy, having the same irradiation coefficient all over the drive cycle. In case of battery charging, the sum $P_{bn}+P_{PV}$ defines the power needed from the ICE to charge the battery (naturally through P_{eg}). If $P_{bn}+P_{PV}<0$, the $\frac{|P_{bn}+P_{PV}|}{P_{eg}}$ will represent the ratio of the power that is divided between the battery and the EM. This ratio is an approximation, since the static characteristics of the EG are non-linear.

Define the equivalent fuel rate used for charging the battery as (8)

$$\dot{m}_{fb} = \frac{|P_{bn}+P_{PV}|}{P_{eg}} \dot{m}_f \quad (8)$$

where $\dot{m}_f$ is the total fuel rate, and $\dot{m}_{fb}$ the equivalent fuel rate for battery charge. The SOC is modified with this value,

namely:

$$\frac{\dot{m}_{fb}}{\frac{dSOC}{dt}} = \frac{\frac{dm_{fb}}{dt}}{\frac{dSOC}{dt}} = \frac{dm_{fb}}{dSOC} \tag{9}$$

The time mean value of (9) is calculated during the simulation, which represents the average amount of consumed fuel per SOC unit:

$$\overline{\frac{dm}{dSOC}} = \frac{1}{T}\int_0^T \frac{dm}{dSOC}dt \tag{10}$$

The fuel amount needed for charging the battery (or fuel excess, respectively) is finally defined by:

$$m_{fb-needed} = \overline{\frac{dm}{dSOC}}(0.7 - SOC_{final}) \tag{11}$$

Where SOC_{final} represents the SOC level at the end of the simulation. Using this fuel equivalent, some performance indices of a control solution can be evaluated.

V. Model Predictive Control for Fuel Consumption Minimization

An attractive solution for optimal control is Model Predictive Control (MPC), which can handle constraints of the inputs, outputs and states as well. MPC was proposed for hybrid vehicles in the literature by different authors, see for example [16]. MPC had spread significantly during the past years in industry as well, due to the computational capacity of nowadays machines [17],[18],[19].

A quadratic cost function is defined for fuel consumption minimization, in the form of:

$$J(k) = \sum_{i=1}^{N} \left\| \hat{y}(k+i|k) - r(k+i|k) \right\|^2 Q(i) + \sum_{i=0}^{N_u} \left\| \Delta\hat{u}(k+i|k) \right\|^2 R(i) \tag{12}$$

Where $\hat{y}(k+i|k)$ are the predictions at time k of the output y, $r(k+i|k)$ is the reference trajectory vector, $\Delta\hat{u}(k+i|k)$ are the changes of the future input vector.

The choice of the weighting factors, prediction and control horizon is crucial, the aim is to get a balance between good tracking and acceptable control signals [20]. As a starting point it is advisable to normalize all signals in the cost function, and then start systematically tuning each element of the diagonal matrices Q and R so that a desired trade-off is achieved.

In what follows, simulation results are presented concerning different tuning parameter values. The reference signals in all cases are: r_1 – drive power demand calculated from the drive cycle, $r_2 = 0.7$ SOC value, $r_3=0$ for fuel rate.

The P_d drive power demand is calculated from the time-velocity characteristics from figure 5, based on the following basic dynamical relations of vehicle motion:

$$\begin{aligned} &P_d(t) = \omega(t) \cdot M_d(t) \\ &\omega(t) = \frac{f_r}{w_r} v(t) \quad , \quad M_d(t) = \frac{w_r}{f_r} F_d(t) \\ &F_d(t) = m \cdot \dot{v} + \frac{1}{2}\rho v^2(t) \cdot A_d \cdot C_d + m \cdot g \cdot C_r \end{aligned} \tag{13}$$

where ω is the angular velocity, M_d - the torque required from the EM, $v(t)$ - the velocity, $\dot{v}(t)$ - the acceleration, m - the vehicle mass. Numerical data regarding these elements, and for the constants A_d, C_d, C_r, g, w_r, ρ are done in [6].

The prediction horizon was $N=10$ and control horizon $N_u=4$ for all simulation cases. For getting conclusive results, the Q and R matrices fixed for three simulation examples.

- The first experiment (figures 6 to 9):

$$Q = \begin{bmatrix} 10^{-2} & 0 & 0 \\ 0 & 100 & 0 \\ 0 & 0 & 0.001 \end{bmatrix}, \quad R = \begin{bmatrix} 10^{-4} & 0 \\ 0 & 10^{-4} \end{bmatrix} \tag{14}$$

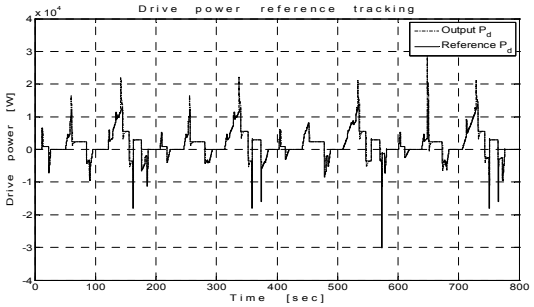

Fig. 6. Drive power reference tracking

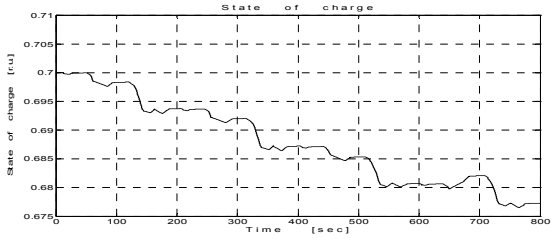

Fig. 7. State of Charge

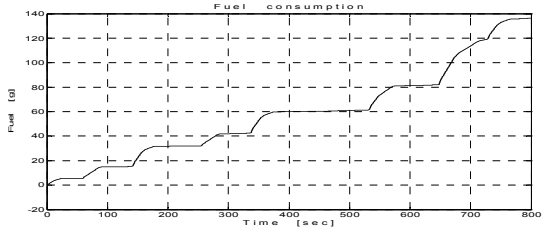

Fig. 8. Fuel consumption

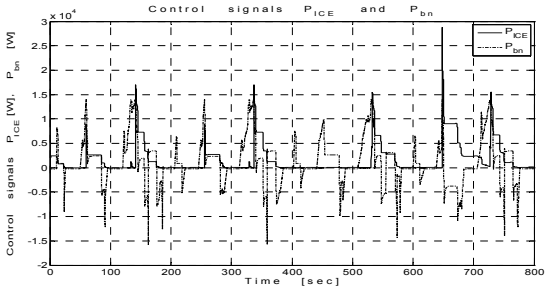

Fig.9. Control signals P_{ICE} and P_{bn}

Synthesising the simulation results, one gets:
- The total fuel consumption is m_f=136.4328g;
- the final SOC is SOC_{final}=0.6773;
- the fuel needed for bringing the SOC to 0.7 following the drive tendency: $m_{fb\text{-}needed}$=79.8137g;
- $m_{total}=m_f+m_{fb\text{-}needed}$=216.2465g.

- The second experiment (figures 10 to 13):

$$Q=\begin{bmatrix} 10^{-3} & 0 & 0 \\ 0 & 100 & 0 \\ 0 & 0 & 0.001 \end{bmatrix},\quad R=\begin{bmatrix} 10^{-5} & 0 \\ 0 & 10^{-5} \end{bmatrix} \qquad (15)$$

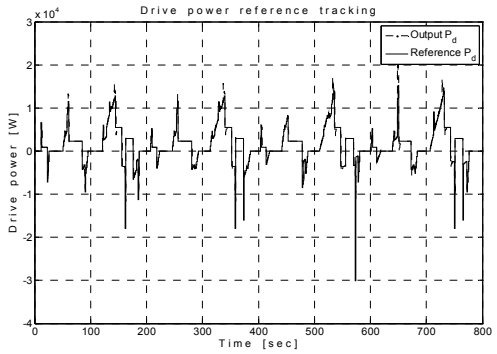

Fig. 10. Drive power reference tracking

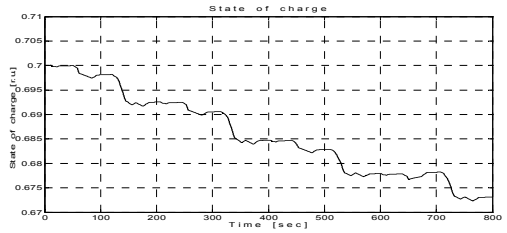

Fig. 11. State of Charge

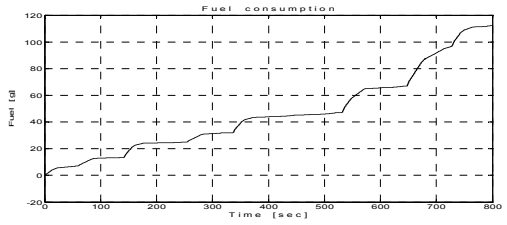

Fig. 12. Fuel consumption

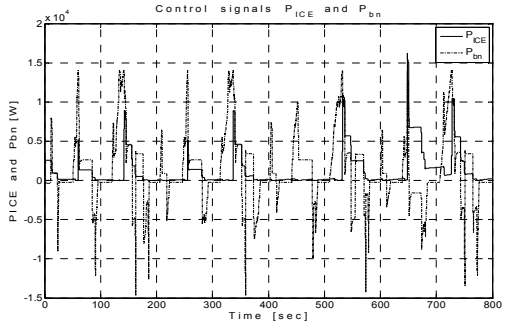

Fig.13. Control signals P_{ICE} and P_{bn}

Synthesising the simulation results, one gets:
- The total fuel consumption is m_f=112.2535g;
- the final SOC is SOC_{final}=0.6731;
- the fuel needed for bringing the SOC to 0.7 following the drive tendency: $m_{fb\text{-}needed}$= 150.8056g;
- $m_{total}=m_f+m_{fb\text{-}needed}$=263.0591g.

- The third experiment (figures 14 to 17)

$$Q=\begin{bmatrix} 10^{-4} & 0 & 0 \\ 0 & 1000 & 0 \\ 0 & 0 & 0.001 \end{bmatrix},\quad R=\begin{bmatrix} 10^{-5} & 0 \\ 0 & 10^{-5} \end{bmatrix} \qquad (16)$$

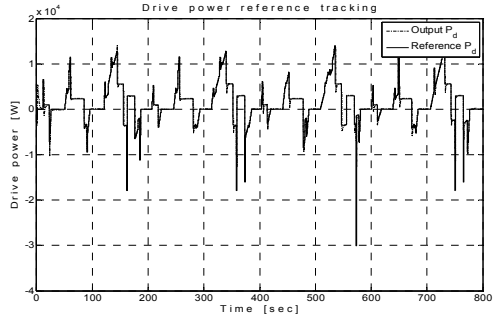

Fig. 14. Drive power reference tracking

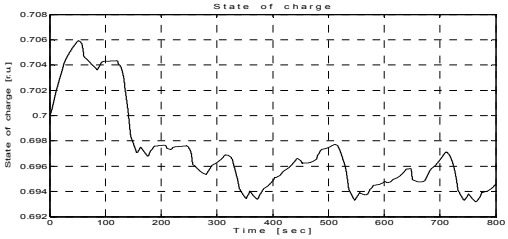

Fig. 15. State of Charge

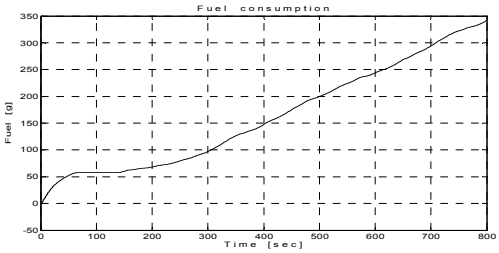

Fig. 16. Fuel consumption

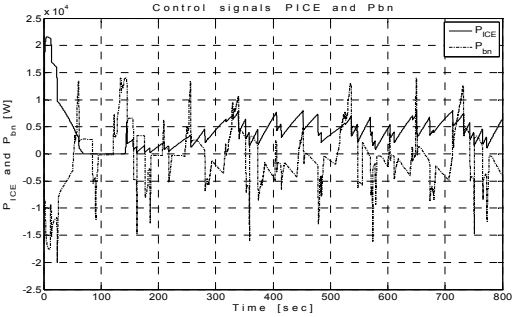

Fig.17. Control signals P_{ICE} and P_{bn}

Synthesising the simulation results, one gets:
- The total fuel consumption is m_f=341.3378g;
- the final SOC is SOC_{final}=0.6946;
- the fuel needed for bringing the SOC to 0.7 following the drive tendency: $m_{fb\text{-}needed}$=77.7170g;
- $m_{total}=m_f+m_{fb\text{-}needed}$=419.0548g.

A simulation was performed for HSV model without any controller at all, when the ICE delivers all the energy needed

for the EM. In this case the total fuel consumption was $m_f=274.7437g$.

Based on the simulation results it can be concluded that for all tuning parameters the total fuel consumed, including the fuel equivalent, gives a value larger than the global optimum. The smallest total fuel is in the case of the first simulation, namely $m_{total}=216.2465g$. This value is smaller than the value without controller. Also in the second case the total fuel is smaller than this value: $m_{total}=263.0591g$, which reflects also an acceptable result.

In this case the tracking performances regarding P_d are good, the overshoots have values between the two other simulations. For the third simulation the tracking is best of all three, with an exception at the start. But the fuel consumption is extremely large, compared to the other cases, it is bigger than the value without controller. This case is not acceptable, it is a good counterexample.

The final values of the SOC largely differ in the first two cases from the third one, reflecting the influence of the tuning weights.

The control signals differ slightly in aspect in the first two cases from the third one. It can also be noticed a difference in the fuel consumption, in the first two cases there is a step-wise evolution (meaning there is no fuel consumption at those moments), whereas in the third one there is an almost continuous and gradual increase, ICE functioning at full load. All these differences reflect the importance of proper balancing of the tuning parameters, which defines the switching between the energy sources.

VI. CONCLUSIONS

The paper presents two solutions for fuel consumption optimization of a series Hybrid Solar Vehicle (HSV), preceded by a brief modelling of the plant.

The first control strategy is dynamic programming, resulting in a global optimum for fuel consumption. For this case the total fuel is calculated and compared with Model Predictive Control results, which is the second control strategy implemented.

Simulations were performed for a reference drive cycle, namely for the urban part of the New European Drive Cycle. Three parameter configurations were chosen, for which reference tracking and fuel consumption minimization give promising results, reflecting the influence on the tuning weights upon the performance of the system. The test simulations presented in the paper were performed using the Matlab/Simulink environment. Future work will concentrate on mathematical model improvement and use of other control strategies.

VII. ACKNOWLEDGEMENTS

This work was supported by the Hungarian National Office for Research and Technology through the project ”Advanced
Vehicles and Vehicle Control Knowledge Center” (ref. number NKTH RET04/2004), which is gratefully acknowledged. The authors also gratefully acknowledge the contribution of Hungarian National Science Foundation (OTKA #K60767).

REFERENCES

[1] Arsie I., M.Graziosi, C.Pianese, G.Rizzo, M. Sorrentino (2004). Optimization of Supervisory Control Strategy for Parallel Hybrid Vehicle with Provisional Load Estimate, *AVEC '04* (Department of Mechanical Engineering – University of Salerno).

[2] G.Maggetto, J. van Mierlo (2001). Electric vehicles, hybrid electric vehicles and fuel cell electric vehicles: state of the art and perspectives, *Ann. Chim. Sci. Mat*, **Vol. 26(4)**, pp. 9-26.

[3] Letendre S., Perez R., Herig C. (2003), Vehicle Integrated PV: A Clean and Secure Fuel for Hybrid Electric Vehicles, Proc. of the American Solar Energy Society Solar 2003 Conference, June 21-23, 2003, Austin,TX.

[4] Arsie I., Rizzo G., Sorrentino M., (2006), Optimal Design of a Hybrid Solar Vehicle, AVEC06 - 8th Intl. Symp. on Advanced Vehicle Control AVEC06, - August 20-24, 2006 – Taipei (TW).

[5] Simpson A., Walker G., Greaves M., Finn D. and Guymer B., (2002) “The UltraCommuter: A Viable and Desirable Solar-Powered Commuter Vehicle”, Australasian Universities Power Engineering Conference, AUPEC’02, Melbourne, Sep 29 – Oct 2, 2002.

[6] P.Bauer, Zs. Preitl, T. Peter, P. Gaspar, Z. Szabo, J. Bokor (2006). Control oriented modelling of a series hybrid solar vehicle, *Workshop on Hybrid Solar Vehicles*, November 6, 2006, University of Salerno, Italy.

[7] R.M. Crowder (1998). *Electric Drives and their Controls*, Oxford University Press Inc., New York.

[8] M. Ehsani, K.M. Rahman, M.D. Bellar, A.J. Severinsky (2001). Evaluation of Soft Switching for EV and HEV Motor Drives, *IEEE Transactions on Industrial Electronics*, **Vol. 48, No.1**, February 2001, pp.82-90.

[9] M.W.T. Koot, J.T.B.A. Kessels, A.G. de Jager, W.P.M.H. Heemels, P.P.J. van den Bosch, M. Steinbuch (2005). Energy Management Strategies for Vehicular Electric Power Systems, *IEEE Trans. on Vehicular Technology*, **54**(3), 771-782.

[10] G.Gutmann (1999*). Hybrid electric vehicles and electrochemical storage systems – a technology push – pull couple, Journal of Power Sources,* **Vol. 84***, pp. 275-279, 1999.*

[11] S. Piller, M. Perrin, A. Jossen (2001*). Methods for state-of-charge determination and their applications*, Journal of Power Sources*, **Vol. 96**, pp. 113-120.*

[12] Egiziano, L.; Femia, N.; Granozio, D.; Petrone, G.; Spagnuolo, G., Vitelli, M., (2006), “Performance Improvement Of Maximum Power Point Tracking Perturb And Observe Method”, Proc. of IASTED Intl. Conf. on Advanced Technology in the Environmental Field (ATEF 2006), Lanzarote, Spain, February 06-08, 2006.

[13] Preitl, Zs., P. Bauer, J. Bokor (2006). Fuel Consumption Optimization for Hybrid Solar Vehicle, *Workshop on Hybrid Solar Vehicles*, November 6, 2006, University of Salerno, Italy.

[14] Andreas Schell, Huei Peng, Doanh Tran, Euthie Stamos, Chan-Chiao Lin, Min Joong Kim (2005). Modelling and control strategy development for fuel cell electric vehicles, *Annual Reviews in Control,* **Vol. 29**, pp. 159-168. (Science Direct)

[15] C. Musardo, G. Rizzoni, Y.Guezennec, B. Staccia (2005). A - ECMS: An Adaptive Algorithm for Hybrid Electric Vehicle Energy Management, *European Journal of Control*, **11 (4-5)**, pp. 509-524.

[16] Back M., M. Simons, F. Kirschaum, V. Krebs (2002). Predictive Control of Drivetrains, *IFAC 15th Triennial World Congress*, Barcelona, Spain.

[17] E.F. Camacho, C. Bordons (1999). *Model Predictive Control*, Springer Verlag London Ltd.

[18] J.M. Maciejowski (2002). *Predictive Control with Constraints,* Pearson Education Ltd.

[19] B. Kulcsar, J. Bokor (2006). Measured Disturbance Estimation for Model Predictive Controller, *Mediterranean Journal of Measurement and Control*, **Vol 2., No 3**, July 2006.

[20] J.A. Rossiter (2003). *Model-Based Predictive Control. A Practical Approach,* CRC Press LLC.